The Disperse Charge-Carrier Kinetics in Regioregular Poly(3-hexylthiophene)

Gerald Dicker,*,† Matthijs P. de Haas,† John M. Warman,† Dago M. de Leeuw,‡ and Laurens D. A. Siebbeles†

Radiation Chemistry Department, IRI, Delft University of Technology, Mekelweg 15, 2629 JB Delft, The Netherlands, and Philips Research Laboratories, Prof. Holstlaan 4, 5656 AA Eindhoven, The Netherlands

Received: July 15, 2004; In Final Form: September 6, 2004

The pulse-radiolysis time-resolved microwave conductivity (PR-TRMC) is an electrodeless technique to measure the transient conductivity in bulk samples induced by a nanosecond high-energy electron pulse. By using the PR-TRMC technique, two commercial samples of regioregular poly(3-hexylthiophene) (P3HT), obtained from Merck and Sigma-Aldrich, were measured as a function of temperature (between 170 and 380 K) and radiation dose. The real part of the high-frequency GHz charge-carrier mobility sum was found to be 0.014 cm^2/V s at room temperature with an activation energy of 28 meV. The conductivity in the Aldrich sample decayed rapidly, with a half-life of 4 ns, while the conductivity of the Merck sample had a half-life of 0.2 μs at room temperature. From measurements of the background conductivity under atmospheric conditions and using the charge-carrier mobility of 0.014 cm^2/V s, a hole doping concentration of 5×10^{17} cm^{-3} (with an activation energy of 61 meV) was found for the Aldrich sample, while it was only 2×10^{16} cm^{-3} (with an activation energy of 98 meV) for the Merck sample. For radiation pulses generating a higher initial electron−hole pair concentration than the doping level, second-order electron−hole recombination was observed in the Merck sample, while in the Aldrich sample, the decay was first-order at all applied doses. This is attributed to the high doping concentration in the latter sample, which exceeded the highest possible pulse-generated electron−hole pair concentration. All transients were of the stretched exponential type (Kohlrausch law). The stretch parameter β increased linearly with temperature in both samples, according to $\beta = T/T_0$ with $T_0 = 930$ and 670 K for Merck and Aldrich P3HT, respectively. The linear increase of β with temperature is in accordance with a model of dispersive hole transport with an exponential distribution of the activation energy of the hopping rates. A generalized version of the Kohlrausch law is derived to include both first- and second-order recombination processes at high radiation doses.

I. Introduction

Various techniques are available, and have been used, to study the mobility, relaxation, and decay of charge carriers in regioregular poly(3-hexylthiophene) (P3HT) and many other conjugated polymers. These techniques include time-of-flight[1−4] (TOF), field-effect transistor[5−8] (FET), photoconductivity[9] (PC), and photoinduced absorption[10−12] (PA) measurements. In TOF measurements, the charge-carrier drift mobility is determined under the action of an electric field. The frequently observed time-dependence of the drift mobility can be related to energetic relaxation of the charge carriers during their "flight" to the counter electrode, where they are neutralized. In FET measurements, the charge-carrier mobility as a function of the gate-induced doping concentration is obtained. In PC measurements, the combined relaxation and recombination of charge carriers, conventionally photogenerated under the influence of a static dc field, is observed. In PA measurements, the recombination of the charge carriers is related to the decay of the photoinduced absorption. These techniques have proven to be very powerful tools to study the mobility, relaxation, and recombination of charge carriers in conjugated polymers. However, some difficulty as to the interpretation of the data arises because of the presence of high dc electric fields used in TOF, FET, and PC measurements. While this is not the case in the (electrodeless) PA technique, ambiguity as to the nature of the detected species (charged or uncharged, free or Coulombically bound) can arise.

The PR-TRMC[13,14] technique circumvents these problems: It is free of electrodes or dc fields; instead, charge carriers are detected by the attenuation of microwaves (at ca. 30 GHz) at a very low (<100 V/cm) field strength, thereby minimally perturbing the diffusive motion and recombination of the charge carriers. The charge-carrier pairs are free of their mutual Coulombic attraction, because they are produced by a high-energy (3-MeV) electron pulse, which uniformly ionizes the bulk sample. The main disadvantage of the PR-TRMC technique is that the contribution of positive and negative charge carriers to the conductivity cannot be distinguished. However, because the negative charge carriers are found to be immobile in most conjugated polymers, the conductivity can almost entirely be ascribed to the mobile holes. In addition, the background (dark) concentration of holes can be measured, which provides an estimate of the concentration of electron-accepting impurities. These are inevitably present in conjugated polymers because of the synthetic routes used and the presence of atmospheric oxygen, and as we show in this article, they can markedly determine the survival time of the charge carriers.

In this work, we apply the PR-TRMC technique to investigate the mobility and recombination kinetics of charge carriers as a function of temperature, impurity, and charge-carrier pair concentration in regioregular P3HT. This polymer is of funda-

* Corresponding author. E-mail address: dicker@iri.tudelft.nl.
† Delft University of Technology.
‡ Philips Research Laboratories.

10.1021/jp046853l CCC: $27.50
Published on Web 10/21/2004

mental, as well as industrial, interest, serving as the active material in prototype polymer electronic devices.[15−17] It is a representative of the whole class of hole-conducting conjugated polymers but stands out because of its high field-effect charge-carrier mobility,[5,18] self-assembling properties,[5,19] and high intrinsic charge-carrier photogeneration efficiency.[20] From the results presented in this paper, we draw important conclusions about the hole relaxation and recombination mechanisms in this polymer.

II. Experimental Section

A. Materials. The polymer used was head-to-tail−head-to-tail coupled regioregular poly(3-*n*-hexylthiophene), P3HT. The two commercial samples of P3HT investigated, from Sigma-Aldrich and Merck, were used without further purification. The Aldrich sample was synthesized via the Rieke route[21] and had a weight-average molecular weight of 87 kg/mol. The Merck sample was synthesized via the McCullough route[22] and had a weight-average molecular weight of 40 kg/mol.

A full comparison of the two synthetic routes, both of which lead to polymers with a regioregularity larger than 98% and a polydispersion index (PDI) of ca. 1.4, has been given elsewhere.[23] The much higher background conductivity found in the present work for the Sigma-Aldrich sample indicates the presence of a residual electron-affinic impurity in this material. We leave the discussion of the potential impurity involved to those more familiar with the synthetic and purification procedures involved.

B. Sample Preparation. Samples were prepared by compressing the polymeric material by hand into a rectangular microwave cell using a close-fitting PTFE rod. The cell consisted of a 14-mm-long piece of copper waveguide with an internal cross section of 3.55×7.1 mm^2 which was closed at one end by a metal plate (short-circuit) and flanged at the other end for connection to the microwave circuitry. The cell was gold-plated using Atomex solution (Engelhard Industries).

The length (ca. 10 mm) and weight (ca. 150 mg) of the sample were accurately measured and used to calculate the fraction, F, of the sample volume actually consisting of bulk solid, taking a density of 1 g/cm^3. The value of F, which invariably lay between 0.5 and 0.7, was used to correct the radiation-induced conductivity for the fact that the sample volume was not completely filled.

The cell was attached to the waveguide circuitry inside a cryostat that was capable of covering a temperature range from −100 to +200 °C. The temperature was regulated by a thermocouple in contact with the cell.

In addition to the time-resolved pulse radiolysis experiments, the dark or background microwave conductivity of the samples was also routinely measured.

C. PR-TRMC Measurements. The PR-TRMC technique and method of data analysis have been described in detail in other publications,[13,14] and a detailed account is provided as Supporting Information to this paper. Only a brief description is, therefore, given in what follows.

The polymer sample inside the microwave cell is uniformly ionized with a single (0.3−50-ns duration) pulse of 3 MeV electrons from a Van de Graaff accelerator. Any change in the conductivity of the sample resulting from the formation of mobile charge carriers, $\Delta\sigma$, is monitored as a decrease in the microwave power reflected by the sample. The microwave frequency range used was 27−38 GHz, and the maximum electric field strength within the sample was ca. 10 V/cm.

The transient change in conductivity could be monitored on a linear time scale for ca. 100 ns after the pulse, with a rise time of ca. 1 ns, or on a logarithmic time scale from tens of nanoseconds to tens of microseconds using a single pulse. The magnitude of $\Delta\sigma$ at the end of the pulse, $\Delta\sigma_{eop}$, provides information on the mobility of the charge carriers formed, and the after-pulse decay of $\Delta\sigma$ provides information on the decay of the mobile carriers via trapping and/or recombination.

The value of $\Delta\sigma_{eop}$ is related to the concentration of charge-carrier pairs formed within the pulse, $n_p(0)$, and the sum of the positive and negative charge-carrier mobilities, $\sum\mu$, by

$$\Delta\sigma_{eop} = qn_p(0)W_{eop}\sum\mu \tag{1}$$

where q is the elementary charge and W_{eop} is the fraction of initially-formed charge-carrier pairs that survive to the end of the pulse. The value of $n_p(0)$ can be calculated from the energy absorbed per unit volume of the sample, D_v, which is accurately known from dosimetry, and the average energy required per ionization event, E_p.

$$n_p(0) = D_v/E_p \tag{2}$$

Substitution for $n_p(0)$ in eq 1 and rearrangement results in the following expression for $\sum\mu$ in terms of the dose-normalized conductivity

$$\sum\mu = \frac{[\Delta\sigma_{eop}/D_v]E_p}{qW_{eop}}. \tag{3}$$

Because the survival probability has a maximum value of unity, a minimum value of the sum of the mobilities of the charge carriers, $\sum\mu_{min}$, can be determined from

$$\sum\mu_{min} = [\Delta\sigma_{eop}/D_v]E_p/q \tag{4}$$

if E_p is known. The value of $E_p = 11$ eV used for P3HT in the present work was derived using the Alig formula[24] (see Supporting Information).

We note that the value of W_{eop} is determined to a large extent by the average thermalization distance of electrons from their sibling positive ion, $\langle r_{th}\rangle$, and the diffusional escape probability of charges separated by this distance. In (high-energy) irradiated organic materials, $\langle r_{th}\rangle$ has been found to be close to 5 nm, and escape probabilities are usually between 1% and 10% at room temperature for low-dielectric-constant hydrocarbon media.[25] This distance is considerably longer than the interchain distance of ca. 1 nm in P3HT. There is, therefore, a high probability that the electron and hole of an initial charge-carrier pair find themselves on different, widely separated polymer chains. Because of this, we believe that the survival probability on a nanosecond time scale in P3HT will be at least 10% and possibly closer to unity. We consider it, therefore, extremely unlikely that the actual values of the mobility sum would be an order of magnitude larger than the values of $\sum\mu_{min}$ calculated using eq 4.

III. Results and Discussion

In what follows, we are concerned mainly with the transient changes in the conductivity of bulk samples of regioregular P3HT that occur on ionization with a short (0.3−50 ns) pulse of high-energy radiation. As mentioned in the previous section, however, we also routinely measure the dark, background conductivity, σ_0, of the samples being investigated. In view of the surprisingly high value of the background conductivity found for the Aldrich sample, these measurements are considered to

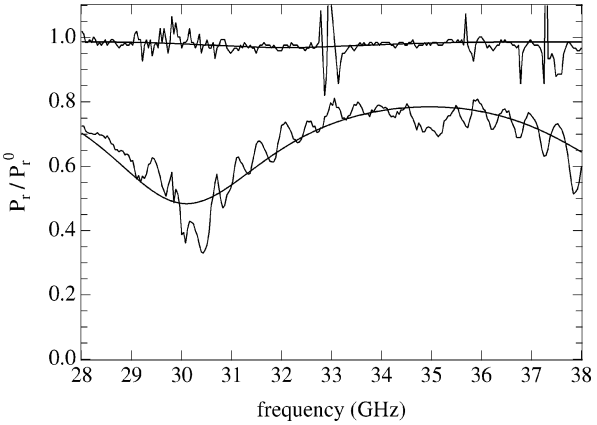

Figure 1. Frequency dependence of the normalized microwave power reflected by a cell containing samples of Merck (upper trace) or Aldrich (lower trace) P3HT at ca. 260 K. The full smooth lines are calculated dependences for background conductivities of 2.7×10^{-5} S/cm (Merck) and 6.8×10^{-4} S/cm (Aldrich).

TABLE 1: Background Conductivity, σ_0, as a Function of Temperature, *T*, for Merck and Aldrich P3HT

Merck P3HT		Aldrich P3HT	
T (K)	σ_0 (S/cm)	*T* (K)	σ_0 (S/cm)
203	7.0×10^{-6}	188	2.8×10^{-4}
233	1.5×10^{-5}	223	4.0×10^{-4}
263	2.7×10^{-5}	259	6.8×10^{-4}
293	4.0×10^{-5}	314	1.1×10^{-3}
323	5.5×10^{-5}		
353	8.0×10^{-5}		
383	1.0×10^{-4}		

be of sufficient interest that they will be presented first, before turning to the results of the pulse experiments.

A. Background (Dark) Conductivity. In Figure 1 are shown frequency scans of the microwave power reflected by cells containing the two P3HT samples in the absence of irradiation. The much larger absorption of microwave power by the Aldrich sample is a qualitative indication of a substantially larger background conductivity. The values of σ_0 determined from fits to the frequency dependence of P_r/P_r^0, as shown in Figure 1, are listed for different temperatures in Table 1. We attribute this dark conductivity to the presence of an extrinsic, electron-affinic impurity, *A*, which results in an equilibrium concentration of mobile holes, $n_{h^+_0}$, according to

$$A \rightleftharpoons A^- + h^+ \tag{5}$$

Because the band gap is on the order of 10^2 k_BT, the concentration of holes will be equal to the concentration of negatively charged acceptor sites, that is

$$n_{h^+_0} = n_{A^-_0} \tag{6}$$

The corresponding value of σ_0 is given by

$$\sigma_0 = q n_{h^+_0} \mu_+ \tag{7}$$

If we take μ_+ to be 0.014 cm^2/V s (see text to follow), a value of $n_{h^+_0}$ of 5×10^{17} cm^{-3} is required to explain the σ_0 value of 1×10^{-3} S/cm found for the Aldrich sample at room temperature. Because of the equilibrium nature of eq 5, this concentration represents a minimum value for the initial concentration of the impurity *A*.

Because the thiophene unit concentration is approximately 4×10^{21} cm^{-3} (based on a density of 1 g/cm^3 and a molecular weight of 166), this indicates a minimum impurity concentration of 125 ppm monomer units. For the Merck sample, a similar estimate yields a value of $n_{h^+_0} = 2 \times 10^{16}$ cm^{-3}, corresponding to a minimum impurity concentration closer to 5 ppm.

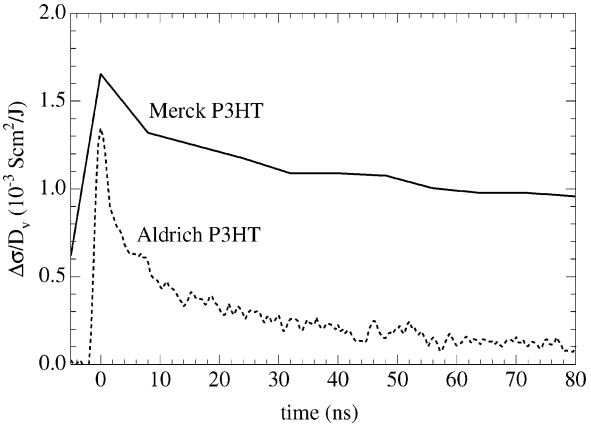

Figure 2. Room-temperature ($T = 293$ K) dose-normalized transient conductivity on irradiation of Merck P3HT (solid line) and Aldrich P3HT (broken line) with a 2-ns pulse.

From Arrhenius-type plots of the background conductivity values shown in Table 1, activation energies of 61 ± 4 meV and 98 ± 2 meV are determined for the Aldrich and Merck samples, respectively. For thermal equilibrium, the activation energy of σ_0 is given to a first approximation by the sum of the activation energy associated with the mobility, ΔE_μ, and half of the energy required for hole formation via reaction 5, ΔE_A, that is

$$\Delta E_\sigma = \Delta E_\mu + \Delta E_A/2 \tag{8}$$

From the values of ΔE_σ and the value of 28 ± 1 meV estimated (in text to follow) for ΔE_μ, ΔE_A values of 66 ± 10 meV and 140 ± 6 meV are derived for the positions of the acceptor sites above the valence band edge in the Aldrich and Merck P3HT samples, respectively.

B. Radiation-Induced Conductivity: Room Temperature. The transient conductivity of Merck P3HT induced by a 2-ns pulse is shown in Figure 2 as the solid line. After an increase during the square pulse, the conductivity decays to two-thirds of its end-of-pulse value within the time axis range of 80 ns. For comparison, the transient conductivity of the Aldrich P3HT sample is shown in the same figure as the broken line. (Note that the apparently higher noise level is due to the faster sampling rate used when recording the Aldrich transient.) The end-of-pulse conductivity is comparable for the two samples, and we obtain for the charge-carrier mobility at room temperature, according to eq 4, $\sum\mu_{min} = 1.4 \times 10^{-2}$ cm^2/V s.

The decay of the conductivity in the Aldrich sample is, however, seen to be much faster than for the Merck sample. This is considered to be further evidence for the presence of a high concentration of an electron-affinic impurity in the former material. On the basis of the background conductivity measured, the equilibrium concentration of holes and negatively charged acceptor sites was estimated to be 5×10^{17} cm^{-3}. This is considerably higher than the concentration of ca. 2×10^{15} cm^{-3} of excess holes and electrons formed in the 2-ns pulse used to obtain the transients in Figure 2. The rapid decay of the conductivity in the Aldrich sample is therefore attributed mainly to the reaction of excess holes with the already present A^- sites via the reverse of reaction 5. This further implies that rapid regeneration of holes via the forward reaction does not occur, and that, under conditions of thermal equilibrium, reaction 5 is displaced mainly to the left (i.e., $n_A \gg n_{h^+_0}$).

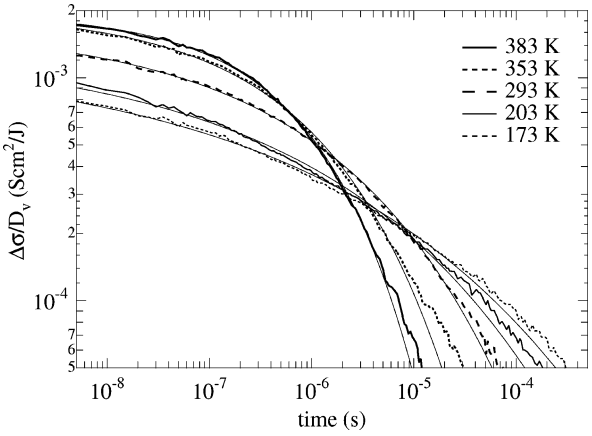

Figure 3. Dose-normalized transient conductivity on pulse irradiation of Merck P3HT at different temperatures using 5-ns pulses. The full smooth curves are least-squares fits using the stretched-exponential expression, eq 9, with the fit parameters given in Table 2.

TABLE 2: For Merck P3HT, the Temperature Dependence of the Charge-Carrier Mobility, $\sum\mu_{min}$, and the Fit Parameters τ and β in the Stretched-Exponential Decay Expression, Eq 9

T (K)	$\sum\mu_{min}$ (cm²/V s)	τ (ns)	β
383	0.019	589	0.47
353	0.018	546	0.37
293	0.014	521	0.27
203	0.009	343	0.20
173	0.007	279	0.17

C. Radiation-Induced Conductivity: Temperature Dependence. Conductivity transients have been measured at various temperatures and recorded over several orders of magnitude in time. For Merck P3HT, the transients are shown in Figure 3 on a double logarithmic scale. As can be seen, the end-of-pulse conductivity increases with increasing temperature, while the lifetime of the charge carriers decreases. All transients in Figure 3 could be fitted using the stretched-exponential (Kohlrausch)[26] expression

$$\Delta\sigma(t) = \Delta\sigma(0)\exp[-(t/\tau)^{\beta}] \quad (9)$$

The fits are shown as the full smooth curves in Figure 3.

We emphasize here that the random diffusional motion of the mobile charge carriers is only minimally perturbed by the low-field-strength (<100 V/cm), ultrahigh-frequency (ca. 30 GHz) microwaves used to probe the conductivity. Charge carriers are therefore not drifted over macroscopic distances to trapping or recombination sites during the time of observation, as can occur in dc measurements.

The values of $\sum\mu_{min}$ determined from $\Delta\sigma(0)$ according to eq 4 are listed in Table 2 together with the other fit parameters τ and β. The charge-carrier mobility, $\sum\mu_{min}$, obeys an Arrhenius-type dependence

$$X = X_0\exp[-E_a/k_BT] \quad (10)$$

as shown in Figure 4. From the straight line fit in Figure 4, the E_a value was found to be 28 meV.

The stretch parameter β was found to be linearly proportional to the temperature, T, as shown in the inset of Figure 4, according to

$$\beta = T/T_0 \quad (11)$$

where T_0 is a characteristic temperature. A straight-line fit

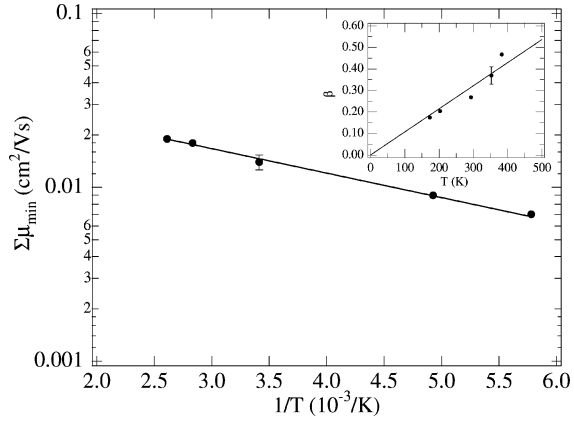

Figure 4. Arrhenius-type plot of the mobility sum, $\sum\mu_{min}$, for Merck P3HT (●). Inset: Fit parameter β in eq 9 vs temperature, T. Values from Table 2.

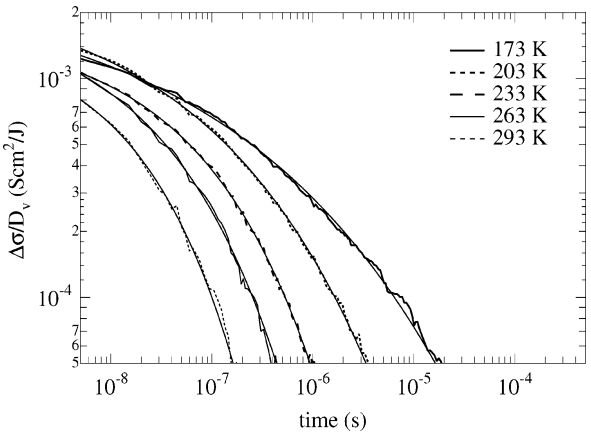

Figure 5. Dose-normalized transient conductivity on pulse irradiation of Aldrich P3HT at different temperatures using 10-ns pulses. The full smooth curves are least-squares fits using the stretched-exponential expression, eq 9, with the fit parameters given in Table 3.

yielded $T_0 = 930 \pm 50$ K. The value of T_0 can be related to the width, $k_BT_0 = 80$ meV, of an exponential distribution of site energies (see the discussion later in the text).

The temperature dependence of the conductivity transients obtained with the Aldrich sample are shown in Figure 5. As can be seen, the conductivity decay is faster at higher temperatures, but in contrast to the Merck sample, the end-of-pulse conductivity decreases as the temperature is raised. We attribute this to fast in-pulse recombination or trapping of the charge carriers at high temperatures. Because of this, the end-of-pulse values cannot be used to derive the temperature dependence of the mobility in this sample. However, at the lowest temperature ($T = 173$ K), the decay is slow enough that an estimate of the charge-carrier mobilty could be obtained and was found to be $\sum\mu_{min} = 0.010$ cm²/V s for this temperature.

As for the Merck sample, all transients could be fitted using the stretched- exponential expression, eq 9. The fits are shown as the full smooth curves in Figure 5, and the fit parameters are listed in Table 3. A straight-line fit to the $\beta(T)$ data according to eq 11 yielded $T_0 = 670 \pm 30$ K, yielding a width of 58 meV for an exponential distribution of site energies.

D. Radiation-Induced Conductivity: Dose Dependence. In Figure 6 are shown conductivity transients for the Merck sample for pulse lengths varying from 0.5 to 50 ns, corresponding to the formation of charge-carrier pairs with concentrations ranging from ca. 5×10^{14} to ca. 5×10^{16} cm^{-3}. Up to ca. 5×10^{15} cm^{-3} (5-ns pulse), the form of the after-pulse decay kinetics

TABLE 3: For Aldrich P3HT, the Temperature Dependence of the Parameters τ and β in the Stretched-Exponential Expression, Eq 9

T (K)	$\sum\mu_{min}$ (cm^2/V s)	τ (ns)	β
293	*a*	11	0.46
263	*a*	16	0.40
233	*a*	35	0.38
203	*a*	18	0.27
173	0.010	17	0.20

[a] In-pulse decay prevented accurate $\sum\mu_{min}$ determination.

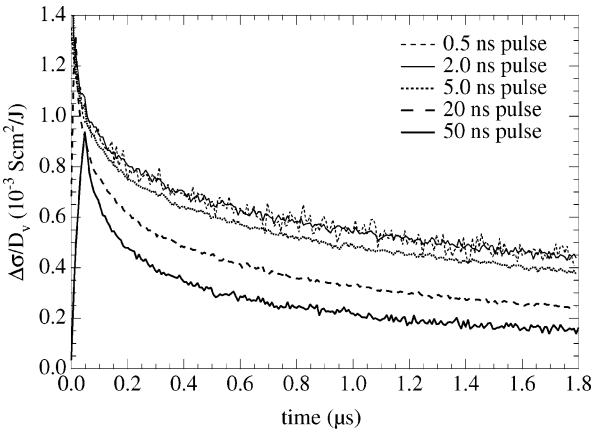

Figure 6. Room-temperature ($T = 293$ K) dose-normalized transient conductivity on irradiation of Merck P3HT with 0.5-, 2-, 5-, 20-, and 50-ns pulses, corresponding to an initial charge-carrier concentration varying from ca. 5×10^{14} to ca. 5×10^{16} cm^{-3}.

is seen to remain almost unchanged. Under these low-dose conditions, therefore, the decay of the conductivity can be ascribed to the reaction of mobile holes with intrinsically present recombination or localization sites, X's. The decay can then be described by the first-order differential rate expression

$$\frac{d\Delta n_{h^+}}{dt} = -k(t) n_X \Delta n_{h^+} \qquad (12)$$

The rate coefficient in eq 12 is taken to be time dependent, because nonexponential, dispersive decay kinetics are, in fact, observed, as shown in the previous section, in which only low-dose results were considered. To explain the stretched-exponential decay given by eq 9, which is found to describe the data very well, the temporal dependence of $k(t)$ must be of the form

$$k(t) = \frac{\kappa}{(\nu t)^{1-\beta}} \qquad (13)$$

with $t > 0$. Comparison of the integrated form of eq 12 with eq 9 shows that $\nu = (\tau\kappa n_X/\beta)^{1/(1-\beta)}/\tau$.

Referring again to Figure 6, we see that, for pair concentrations larger than ca. 1×10^{16} cm^{-3}, a significant increase in the decay rate occurs. We attribute this to the fact that charge recombination between pairs formed in the pulse now provides a substantial additional contribution to the after-pulse decay kinetics. Because, in this case, $\Delta n_{h^+} = \Delta n_{e^-}$, this leads to an additional second-order term in the rate expression

$$\frac{d\Delta n_{h^+}}{dt} = -k(t) n_X \Delta n_{h^+} - h(t) \Delta n_{h^+}^2 \qquad (14)$$

Interestingly, the pair concentration at which the second-order term becomes important is close to the intrinsic hole (and A^-) concentration of 2×10^{16} cm^{-3}, calculated on the basis of the dark conductivity. We conclude that the intrinsic decay at low doses also most probably involves a charge recombination reaction with the negatively charged impurity site, A^-, as the counterion. In view of this, we take the temporal form of $h(t)$ to be the same as that for $k(t)$, which results in

$$\frac{d\Delta n_{h^+}}{dt} = -\frac{1}{(\nu t)^{1-\beta}} (\kappa n_X \Delta n_{h^+} + \gamma \Delta n_{h^+}^2) \qquad (15)$$

Integration of eq 15 leads to the following expression for the time dependence of the excess hole concentration for the combined first- and second-order recombination processes

$$\Delta n_{h^+}(t) = \frac{\Delta n_{h^+}(0) e^{-(t/\tau)^\beta}}{1 + \gamma \Delta n_{h^+}(0)(1 - e^{-(t/\tau)^\beta})/\kappa n_X} \qquad (16)$$

with $\tau = (\beta/\kappa n_X)^{1/\beta} \nu^{1/\beta - 1}$. This is an extension of the Kohlrausch equation to second-order processes. It was used to fit the transients, shown at room temperature on a logarithmic time scale in Figure 7 for the different doses used, keeping the parameters β, τ, κn_X, and γ constant. The values of the parameters found are given in Table 4 for the three temperatures for which a dose dependence was studied.

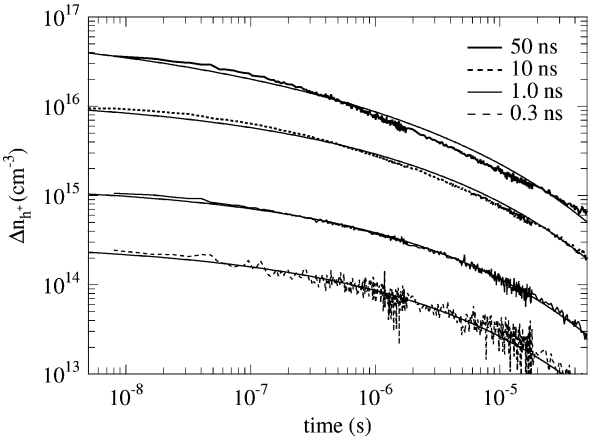

Figure 7. Dose dependence of the charge-carrier decay kinetics for Merck P3HT at $T = 297$ K using electron pulses from 0.3 to 50 ns. The full smooth curves are least-squares fits using eq 16. The fit parameters are given in Table 4.

TABLE 4: For Merck P3HT, the Temperature Dependence of the Fit Parameters τ, β, κn_X, and γ in Eq 16

T (K)	τ (ns)	β	κn_X (10^8 s^{-1})	γ (10^{-8} cm^3/s)
193	296	0.22	2.8	0.38
297	465	0.29	3.7	1.06
397	567	0.42	4.3	2.11

For Aldrich P3HT, the dose-normalized conductivity transients found upon variation of the pulse length are shown in Figure 8. Little difference is found in the height and decay of the conductivity for the shortest (0.5 and 2.0 ns) pulses. However, because of the ca. 10-ns decay time for this sample, the 20- and 50-ns pulse transients tend to level off within the pulse. The after-pulse decay of the conductivity, however, is seen to be independent of the total dose, which varies by 2 orders of magnitude, in contrast to the results for the Merck sample. This is in accordance with the high background value of n_{A^-} of 5×10^{17} cm^{-3}, which is an order of magnitude larger than the concentration of holes and electrons formed even for the maximum pulse-length used. The decay of the conductivity will therefore be controlled mainly by the reaction of holes with the already-present A^- sites, even for the highest dose used.

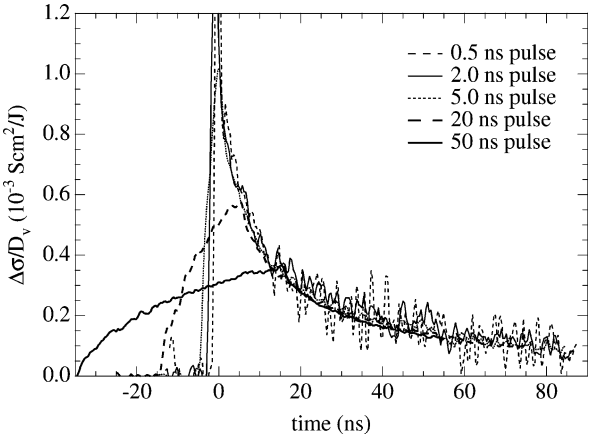

Figure 8. Room-temperature ($T = 293$ K) dose-normalized transient conductivity on irradiation of Aldrich P3HT with 0.5-, 2-, 5-, 20-, and 50-ns pulses, corresponding to an initial charge-carrier concentration varying from ca. 5×10^{14} to ca. 5×10^{16} cm^{-3}.

E. Interpretation of the Stretched-Exponential Decay Law. The time-dependent reaction rate coefficient in the form of eq 13 used to derive the stretched-exponential decay law can be related to the time-dependent dc charge-carrier mobility found in TOF measurements on P3HT[1,3,4,27−29] via Debye's relation,[30]

$$k(t) = \frac{q}{\epsilon_0 \epsilon_r} \mu_{dc}(t) \tag{17}$$

with

$$\mu_{dc}(t) \propto \frac{1}{(\nu t)^{1-\beta}} \tag{18}$$

for $t > 0$. For an exponential distribution of the thermal activation energy of the hopping rates, it was shown that the dispersion parameter β is connected to the width of the distribution, $k_B T_0$ via[31−33]

$$\beta = T/T_0 \tag{19}$$

This dependence has been found already (see inset of Figure 4), and we obtained $k_B T_0 = 80$ and 58 meV for the Merck and Aldrich P3HT, respectively.

The time dependence of the dc mobility of the form of eq 18 found in TOF measurements could imply the same time dependence of the high-frequency charge-carrier mobility sum, $\sum\mu_{min}$, applicable to the present work. Because the conductivity is the product of $\sum\mu_{min}$ and n_p (and the elementary charge), the time dependence of the conductivity should be

$$\Delta\sigma(t) \propto e^{-(t/\tau)^{\beta}}/(\nu t)^{1-\beta} \tag{20}$$

instead of eq 9. We have tried to fit the transients in Figures 3 and 5 using this expression and found that this function did not fit the data accurately. We therefore conclude that, in contrast to the dc mobility, the high-frequency charge-carrier mobility found in the present PR-TRMC is weakly time dependent. This is in agreement with the over-the-barrier (OVB) transport model.[34] In summary, the following picture arises: The present high-frequency technique probes the mobility of the holes within the ordered, conjugated domains. Disappearance of the holes occurs by diffusive recombination at electron-occupied impurities and radiation-induced electrons. Diffusion takes place in an exponentially distributed landscape of energy barriers.

IV. Conclusions

We have applied the PR-TRMC technique to study the charge-carrier recombination in two different samples of regioregular P3HT obtained from Merck and Sigma-Aldrich. We found the charge-carrier mobility sum to be 0.014 cm^2/V s at room temperature with an activation energy of 28 meV. This low activation energy, compared to dc results,[4] must be related to the frequency of detection and reflects the motion of the holes in the ordered domains of the polymer.

The conductivity in the Aldrich sample upon pulsed excitation decayed rapidly, with a half-life of only 4 ns, while the conductivity of the Merck sample had a half-life of 0.2 μs at room temperature. The much faster decay in the Aldrich sample must be due to the 1 order of magnitude higher background conductivity. We conclude that the disappearance of the radiation-induced surplus of holes is given by the recombination (localization) at electron-occupied impurity acceptor sites at low doses. At higher doses, electron−hole recombination is observed.

The decay kinetics of the holes at low doses was found to be appropriately described by the stretched-exponential (Kohlrausch) decay law, with the stretch parameter β increasing linearly with temperature in either sample, according to $\beta = T/T_0$ with $T_0 = 930$ and 670 K for the Merck and Aldrich P3HT, respectively. The linear increase of β with temperature can be ascribed to dispersive hole transport in an exponential density of site energies. The Kohlrausch decay law was extended to second-order processes to fit the high-dose transients.

We have shown that the lifetime of the charge carriers is crucially determined by the concentration of electron acceptors, the magnitude of which is dependent on the synthetic route. For applications of P3HT in field-effect transistors, a high on−off ratio is required. This can only be achieved if the background conductivity, hence acceptor concentration, is minimized. In photon-to-electricity converting devices, it is important that the photoinduced charge carriers survive their diffusional drift to the electrodes, again requiring a low acceptor concentration. Minimizing the acceptor concentration by choosing the appropriate synthesis conditions therefore is important in developing highly efficient devices based on regioregular P3HT.

Acknowledgment. This work is part of the research program of the Stichting voor Fundamenteel Onderzoek der Materie (FOM, financially supported by NWO) and Philips Research.

Supporting Information Available: Detailed description of the PR-TRMC technique. This material is available free of charge via the Internet at http://pubs.acs.org.

Note Added after ASAP Publication. This paper was published on the Web on 10/21/2004 with errors in equations 14 and 15. The corrected version was reposted on 10/28/2004.

References and Notes

(1) Pandey, S. S.; Takashima, W.; Nagamatsu, S.; Endo, T.; Rikukawa, M.; Kaneto, K. *Jpn. J. Appl. Phys.* **2000**, *39*, L94−L97.

(2) Juška, G.; Arlauskas, K.; Österbacka, R.; Stubb, H. *Synth. Met.* **2000**, *109*, 173−176.

(3) Takashima, W.; Pandey, S. S.; Endo, T.; Rikukawa, M.; Tanigaki, N.; Yoshida, K. Y.; Kaneto, K. *Thin Solid Films* **2001**, *393*, 334−342.

(4) Mozer, A. J.; Sariciftci, N. S. *Chem. Phys. Lett.* **2004**, *389*, 438−442.
(5) Sirringhaus, H.; Brown, P. J.; Friend, R. H.; Nielssen, M. M.; Bechgaard, K.; Langeveld-Voss, B. M. W.; Spiering, A. J. H.; Janssen, R. A. J.; Meijer, E. W.; Herwig, P.; de Leeuw, D. M. *Nature* **1999**, *401*, 685−688.
(6) Katz, H. E.; Bao, Z. *J. Phys. Chem. B* **2000**, *104*, 671−678.
(7) Babel, A.; Jenekhe, S. A. *J. Phys. Chem. B* **2003**, *107*, 1749−1754.
(8) Tanase, C.; Meijer, E. J.; Blom, P. W. M.; de Leeuw, D. M. *Phys. Rev. Lett.* **2003**, *91*, 216601.
(9) Takayama, K.; Kaneko, M.; Pandey, S. S.; Takashima, W.; Kaneto, K. *Synth. Met.* **2001**, *121*, 1565−1566.
(10) Österbacka, R.; An, C. P.; Jiang, X. M.; Vardeny, Z. V. *Science* **2000**, *287*, 839−842.
(11) Korovyanko, O. J.; Österbacka, R.; Jiang, X. M.; Vardeny, Z. V.; Janssen, R. A. J. *Phys. Rev. B* **2001**, *64*, 235122.
(12) Westerling, M.; Österbacka, R.; Stubb, H. *Phys. Rev. B* **2002**, *66*, 165220.
(13) Warman, J. M.; de Haas, M. P.; Hummel, A. *Chem. Phys. Lett.* **1973**, *22*, 480−483.
(14) Warman, J. M.; de Haas, M. P. In *Pulse Radiolysis*; Tabata, Y., Ed.; CRC Press: Boca Raton, FL, 1991.
(15) Bao, Z.; Dodapalapur, A.; Lovinger, A. *Appl. Phys. Lett.* **1996**, *69*, 4108−4110.
(16) Sirringhaus, H.; Tessler, N.; Friend, R. H. *Science* **1998**, *280*, 1741−1744.
(17) Stutzmann, N.; Friend, R. H.; Sirringhaus, H. *Science* **2003**, *299*, 1881−1884.
(18) Wang, G.; Swensen, J.; Moses, D.; Heeger, A. J. *J. Appl. Phys.* **2003**, *93*, 6137−6141.
(19) Mena-Osteritz, E.; Meyer, A.; Langeveld-Voss, B. M. W.; Janssen, R. A. J.; Meijer, E. W.; Bäuerle, P. *Angew. Chem., Int. Ed.* **2000**, *39*, 2680−2684.
(20) Dicker, G.; de Haas, M. P.; Siebbeles, L. D. A.; Warman, J. M. *Phys. Rev. B* **2004**, *70*, 45203.
(21) Chen, T.-A.; Wu, X.; Rieke, R. D. *J. Am. Chem. Soc.* **1995**, *117*, 233−244.
(22) McCullough, R. D.; Lowe, R. D. *J. Chem. Soc., Chem. Commun.* **1992**, 70.
(23) McCullough, R. D. In *Handbook of Oligo- and Polythiophenes*; Fichou, D., Ed.; Wiley-VCH: Weinheim, 1999.
(24) Alig, R. C.; Bloom, S.; Struck, C. W. *Phys. Rev. B* **1980**, *22*, 5565.
(25) *Kinetics of nonhomogeneous processes*; Freeman, G. R., Ed.; John Wiley & Sons: New York, **1987**.
(26) Kohlrausch, R. *Annu. Rev. Phys. Chem.* **1854**, *91*, 179.
(27) Nagamatsu, S.; Pandey, S. S.; Takashima, W.; Endo, T.; Rikukawa, M.; Kaneto, K. *Synth. Met.* **2001**, *121*, 1563−1564.
(28) Takashima, W.; Nagamatsu, S.; Pandey, S. S.; Endo, T.; Yoshida, Y.; Tanigaki, N.; Rikukawa, M.; Yase, S.; Kaneto, K. *Synth. Met.* **2001**, *119*, 563−564.
(29) Genevičius, K.; Österbacka, R.; Juška, G.; Arlauskas, K.; Stubb, H. *Synth. Met.* **2003**, *137*, 1407−1408.
(30) Debye, P. *Trans. Electrochem. Soc.* **1942**, *82*, 265.
(31) Pfister, G.; Scher, H. *Adv. Phys.* **1978**, *27*, 747.
(32) Silver, M.; Schönherr, G.; Bässler, H. *Phys. Rev. Lett.* **1982**, *48*, 352−355.
(33) Schnörer, H.; Haarer, D.; Blumen, A. *Phys. Rev. B* **1988**, *38*, 8097−8101.
(34) van de Craats, A. M.; Siebbeles, L. D. A.; Bleyl, I.; Haarer, D.; Berlin, Y. A.; Zharikov, A. A.; Warman, J. M. *J. Phys. Chem. B* **1998**, *102*, 9625−9634.